Losses and orbital part of the Poynting vector of air-core modes in hollow-core fibers

G.K. Alagashev [1], S.S. Stafeev [2], A.D. Pryamikov [1]
[1] Prokhorov General Physics Institute of RAS, 119991, Moscow, Russia, Valilova St. 38;
[2] Image Processing Systems Institute, NRC "Kurchatov Institute", 443001, Samara, Russia, Molodogvardeiskaya St. 151

Abstract

In our earlier works, we investigated a relationship between the formation of vortices in the transverse component of the Poynting vector of core modes and the regimes of strong localization of these modes in solid core micro-structured optical fibers. In this paper, we consider the behavior of the orbital part of the Poynting vector of fundamental and high-order modes in hollow-core fibers, and make comparisons with similar fundamental core mode behavior in solid core micro- structured optical fibers. We then demonstrated the impact of the "negative" curvature of the core-cladding boundary of a hollow-core fiber on the behavior of the orbital part of the Poynting vector of the air-core modes.

Keywords: micro-structured optical fibers, singular optics, core modes, spin and orbital parts of the Poynting vector, light localization.

Citation: Alagashev GK, Stafeev SS, Pryamikov AD. Losses and orbital part of the Poynting vector of air-core modes in hollow-core fibers. Computer Optics 2024; 48 (2): 192-196. DOI: 10.18287/2412-6179-CO-1349.

Introduction

Until recently, micro-structured optical fibers (MOFs) have been studied mainly in terms of transmission and generation of OAM (orbital angular momentum) modes [1]. It is known that there is a huge increase in demand for data transmission capacity, which in turn prompts the search for effective methods to solve the problem of capacity crunch. The use of such multiple space channels as OAM modes provides a new degree of physical dimension for space division multiplexing [2]. In contrast to the spin angular momentum (SAM) of a core mode, which has the values of $\pm\hbar$ depending on left- and right-handed circularly polarized state, OAM of the core mode is related to its helical phase factor $\exp(\pm il\varphi)$ and has the values of $l\hbar$ per photon [3].

Since the first demonstration of an air-core fiber capable of transmitting OAM modes with outstanding stability [4] at a distance of 13.4 km [5], various designs of MOFs capable of transmitting a significant number of OAM modes have been proposed. Among them were hollow-core photonic crystal fibers [6, 7] operating in a wide spectral range. Besides, a spatial division multiplexed optical transmission over a multi-ring-solid core OAM fiber with 56 OAM mode channels over a 60 km span was demonstrated in [8]. Another study, focusing on helically twisted photonic- crystal fibers that preserve the chirality of OAM modes of the same order for possible applications in OAM modes transmission, is also worth mentioning [9].

In the above examples, OAM modes were generated using spatial light modulators, spiral phase plates, fiber gratings and other devices. In this work, we demonstrate that vortex motions of the core mode energy flow in hollow-core MOFs can occur not only when using special devices, but also under the leakage of the core mode energy. It should be noted that such MOFs as all solid band gap fibers [10] and hollow-core fibers [11] are leaky waveguides, unlike step-index fibers used, for example, in telecommunications. The propagation constants of the core modes of the leaky fibers are complex numbers, while for step-index fibers, the radiation propagates according to the principle of total internal reflection, with propagation constants of the core modes being real numbers.

In our previous works [12], we showed that the transverse component of the Poynting vector of the fundamental core mode of both solid-core and hollow-core MOFs has a vortex structure with singularities located at points with coordinates given by the equation $P_x(x,y)=P_y(x,y)=0$, where P_x and P_y are projections of the transverse component of the Poynting vector of the fundamental core mode [13]. These singularities can arise both on the axis of the micro- structured fiber and in its cladding. In addition, for all- solid MOFs, a relationship was found between the vortex structure of the orbital part of the transverse component of the Poynting vector of the fundamental core mode and the region of low losses that occurs in certain ranges of the MOF geometrical parameters in certain spectral bands [14]. It was also demonstrated that it is in fact the orbital part of the transverse component of the Poynitng vector that determines the leakage losses of the fundamental core mode in all-solid MOFs.

In this paper, we consider the behavior of the orbital part of the transverse component of the Poynting vector, not only of the fundamental, but also of high-order mode of the hollow-core fiber. We show that the main deviation of the streamlines of the orbital part of the Poynting vector of the air-core modes from radial direction occurs at the boundaries of the cladding capillaries. In addition, for all solid MOFs, it is the orbital part of the Poynting vector that determines the level of waveguide losses of hollow-core MOFs.

1. Losses and orbital part of the Poynting vector of air-core modes for silica glass capillary

As in the case of all solid dielectric pipes, the spin and orbital parts of the Poynting vector of fundamental air-core mode of a silica glass capillary are determined by the same expressions as in [14]. The difference is that for a silica glass capillary, an effective refractive index of the air-core mode $n_{eff}<1$ in the expressions for the electric and magnetic fields of the air-core mode $\vec{E}=\vec{E}(r,\varphi)e^{i(\omega t-\beta z)}$ and $\vec{H}=\vec{H}(r,\varphi)e^{i(\omega t-\beta z)}$, where ω is the circular frequency, $\beta=2\pi n_{eff}/\lambda$ (λ is a wavelength) and r, φ, z are cylindrical coordinates, respectively. The expressions for the axial components of the hybrid modes fields of the HE type of order n have the following form:

$$E_z = AJ_n(k_t r)F_n(\varphi),\ r<a, \quad (1)$$

$$H_z = BJ_n(k_t r)F_n(\varphi), \quad (2)$$

where a is the radius of the capillary air-core, $k_t^2+\beta^2=k_0^2$ $(k_0=2\pi/\lambda)$, J_n is Bessel function of the first kind and $F_n(\varphi)$ is equal to $\cos(n\varphi)$ or $\sin(n\varphi)$ depending on whether an even or odd air-core mode is considered. In the capillary wall, these expressions can be represented as:

$$E_z = \left(CH_n^{(1)}(k_t r)+DH_n^{(2)}(k_t r)\right)F_n(\varphi),\ a<r<d, \quad (3)$$

$$H_z = \left(GH_n^{(1)}(k_t r)+KH_n^{(2)}(k_t r)\right)F_n(\varphi), \quad (4)$$

where d is a thickness of the capillary wall, $k_t^2+\beta^2=k^2$ $(k=2\pi n_{silica}/\lambda)$ and $H_n^{(1)}$, $H_n^{(2)}$ are Hankel functions of both kinds. Outside the capillary, the axial components of the air-core mode fields are equal:

$$E_z = LH_n^{(2)}(k_t r)F_n(\varphi),\ r>d, \quad (5)$$

$$H_z = MH_n^{(2)}(k_t r)F_n(\varphi), \quad (6)$$

where $k_t^2+\beta^2=k_0^2$ $(k_0=2\pi/\lambda)$.

Based on the expressions obtained for the axial components of the air-core mode fields, we can calculate all other field components in cylindrical coordinates [15] and corresponding expressions for the orbital and spin parts of the transverse component of the Poynting vector [16]:

$$\vec{P}_{transv}=\vec{P}_{transv}^{spin}+\vec{P}_{transv}^{orbit}, \quad (7)$$

$$\vec{P}_{transv}^{spin}=\varepsilon_0 c^2/(4\omega)\vec{\nabla}\times\mathrm{Im}\left(\vec{E}^*\times\vec{E}\right), \quad (8)$$

$$\vec{P}_{transv}^{orbit}=\varepsilon_0 c^2/(2\omega)\mathrm{Im}\left(\vec{E}^*(\vec{\nabla})\vec{E}\right), \quad (9)$$

where $\vec{E}^*(\nabla)\vec{E}=E_x^*\nabla E_x+E_y^*\nabla E_y+E_z^*\nabla E_z$.

In this work, we have studied a silica glass capillary with an air-core diameter of 40 μm and a wall thickness of 750 nm. Using the commercial packet COMSOL (finite element method) and Matlab, we calculated losses of HE_{11} air-core mode (fundamental mode) in the second transmission band for the silica glass capillary (Fig. 1*a*). In addition, we considered the dependences of the orbital part of the transverse component of the Poynting vector on wavelength for HE_{11} air-core mode for linear and circular polarization (Fig. 1*a*). The calculations showed that the orbital part of the transverse component of the Poynting vector of the fundamental air-core mode exactly matches the capillary loss curve, as in the case of an all solid dielectric pipe and all solid micro-structured fibers [14]. This means that for a capillary, it is the orbital part of the transverse component of the Poynting vector that determines the level and behavior of leakage losses.

Fig. 1*b* shows the distribution of the orbital part of the transverse component of the Poynting vector of the HE_{11} air-core mode for linear polarization at a wavelength of 1 μm. As can be seen, the streamlines of the orbital part have the same direction as in the case of a dielectric all solid pipe and they are determined by its radial projection [14]. These findings for leaky waveguides with a round core can be confirmed by analytical calculations [14].

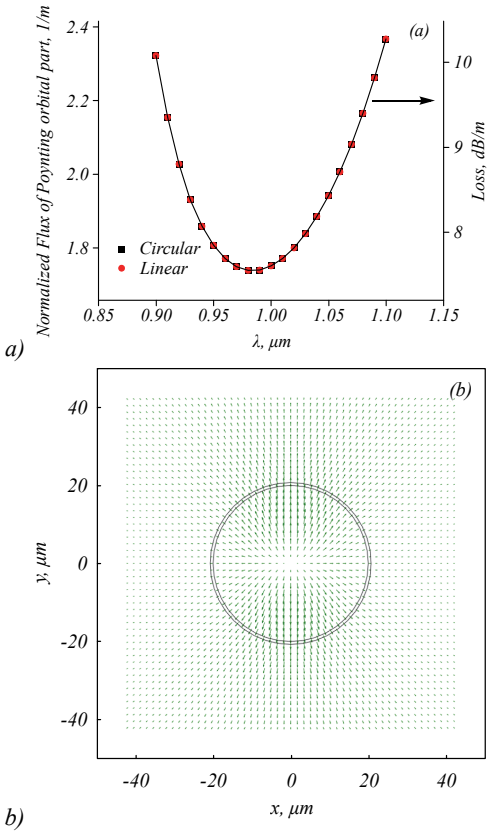

Fig. 1. (a) The dependence of losses and the orbital part of the transverse component of the Poynting vector of the fundamental air-core mode on wavelength in the second transmission band for silica glass capillary described in the text (linear and circular polari-zation of the air-core mode was considered); (b) distribution of the orbital part of the transverse component of the Poynting vector of the fundamental air-core mode of the silica glass capillary for the case of linear polarization at a wavelength of 1 μm

Another important issue is to consider similar distributions for high order air-core modes. For the silica glass capillary, we calculated the distribution of the orbital part of the Poynting vector for the hybrid HE_{21} air-core mode which is

shown in Fig. 2 for both polarizations. It can be seen that for linear polarization of the HE_{21} air-core mode (Fig. 2*a*), the distribution of the orbital part of the transverse component of the Poynting vector has a structure similar to that of the orbital part of the fundamental air-core mode (Fig. 1*b*). Moreover, it can be seen from Fig. 2*a* that the structure of the orbital part of the Poynting vector is determined by the azimuthal dependence of the fields of the HE_{21} air-core mode in the form of $\cos(n\varphi)$ or $\sin(n\varphi)$. For circular polarization of the HE_{21} air-core mode, we can observe a vortex in distribution of the orbital part of the Poynting vector with a singularity on the axis of the capillary. The topological charge of vortex is equal to ±1, as follows from the conclusions of fiber singular optics [17]. It should be noted that the losses for both types of polarizations for the HE_{21} air-core mode were equal to 30 dB/m at a wavelength of 1 μm.

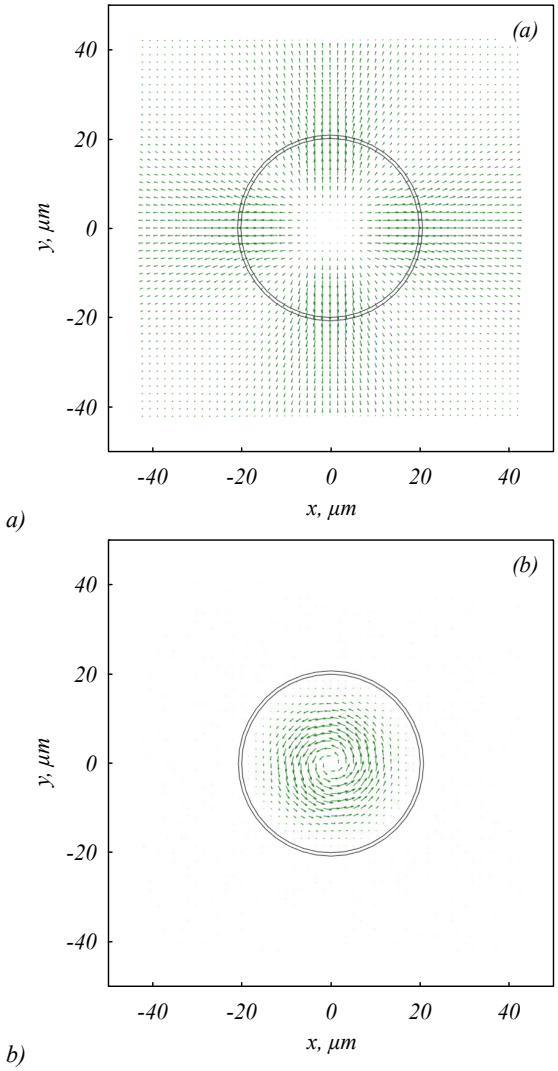

Fig. 2. (a) Distribution of the orbital part of the transverse component of the Poynting vector of HE_{21} air-core mode of the silica glass capillary for the case of linear polarization at a wavelength of 1 μm; (b) distribution of the orbital part of the transverse component of the Poynting vector of HE_{21} air-core mode of the silica glass capillary for the case of circular polarization at a wavelength of 1 μm

2. Losses and orbital part of the Poynting vector of air-core modes for silica glass hollow-core fiber

Let us consider similar dependences and distributions of losses and orbital parts of the Poynting vector of air-core modes of silica glass hollow-core fiber with a more complex cladding design [11] (Fig. 3). For this, a hollow-core fiber with a cladding consisting of eight silica glass capillaries with a wall thickness of 750 nm was considered. The air-core diameter was 40 μm.

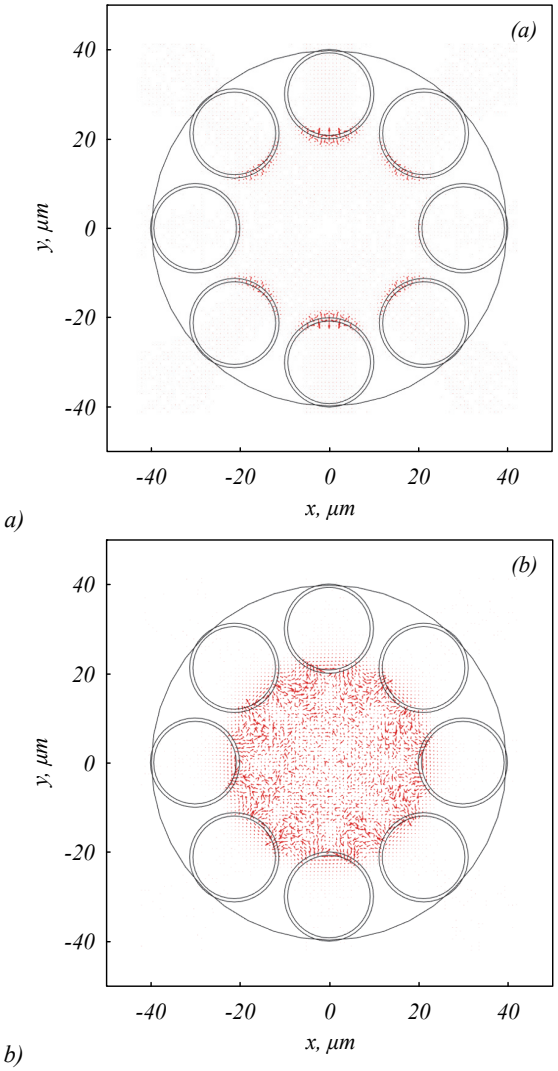

Fig. 3. (a) Distribution of the orbital part of the transverse component of the Poynting vector of HE_{11} air-core mode of the silica glass hollow-core fiber for the case of linear polarization at a wavelength of 1 μm; (b) distribution of the orbital part of the transverse component of the Poynting vector of HE_{11} air-core mode of the silica glass hollow-core fiber for the case of circular polarization at the same wavelength

Fig. 3 shows the distributions of the orbital parts of the transverse components of the Poynting vector of the HE_{11} air-core mode (fundamental mode) for linear and circular polarizations at a wavelength of 1 μm. It can be seen that the structure of the orbital part of the Poynting vector is fundamentally different from the similar structure of the orbital part for the silica glass capillary

(Fig. 1*b*). A strong interaction is observed at the boundaries of cladding capillaries for linear polarization of the HE_{11} air-core mode (Fig. 3*a*). For both polarizations, the distribution of the orbital part of the Poynting vector of the fundamental air-core mode has a much more complex vortex structure at the core-cladding boundary in contrast to the same distributions for the silica glass capillary. The maximum deviation of the vector of the orbital part of the transverse component of the Poynting vector from the radial direction occurs precisely at the boundaries of the cladding capillaries, which is associated with the so-called "negative" curvature of the core-cladding boundary [11].

However, the dependence of the orbital part of the Poynting vector on wavelength exactly coincides with the dependence of loss on wavelength for a hollow-core fiber (Fig. 4) as well as for the same dependence for the silica glass capillary (Fig. 1*a*). As in the case of solid-core MOFs [14], it can also be argued that the spin part of the Poynting vector of the air-core modes has a very small effect on the loss level and the shape of the loss curve of hollow-core fibers. It is the orbital part of the transverse component of the Poynting vector that plays a decisive role in the loss formation in the hollow-core fibers.

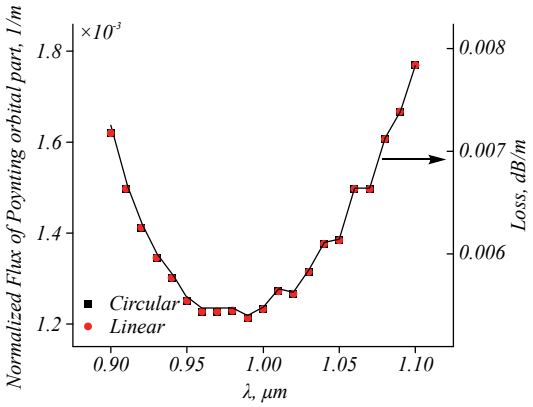

Fig. 4. The dependence of losses (solid curve) and the orbital part of the transverse component of the Poynting vector (squares and circles) of the fundamental air-core mode on wavelength in the second transmission band for silica hollow-core fiber described in the text (linear and circular polarization of the air-core mode was considered)

Fig. 5 shows the distributions of the orbital parts of HE_{21}mode of the hollow-core fiber. Here, as in the case of HE_{11} mode, we can see a strong interaction of the orbital part of the transverse component of the Poynting vector with the cladding capillaries for linear polarization and a vortex structure of the orbital part for circular polarization with a singularity on the fiber axis. The losses for both types of polarizations for the HE_{21} air-core mode were equal to 0.075 dB/m at a wavelength of 1 μm.

Conclusions

In this work, we have considered the behavior of the orbital part of the transverse component of the Poynting vector of air-core modes in a silica glass capillary and in a silica glass hollow-core fiber with a cladding consisting of eight capillaries. It was demonstrated that the dependences of the orbital part of the Poynting vector of the air-core modes on wavelength are identical to the loss dependences on wavelength for these fibers. The same relationship was demonstrated for all solid micro-structured fibers in our earlier work [14]. As can be seen from Fig. 1*a* and Fig. 4, the loss level in a silica glass capillary is approximately 1000 times greater than the one in a hollow-core fiber with a "negative" curvature of the core-cladding boundary. All parameters of the fibers were chosen to be the same, and the calculations were carried out for the same transmission band. There is a qualitative difference in the behavior of the orbital part of the transverse component of the Poynting vector of the air-core modes precisely at the core-cladding boundary for both types of the hollow-core fibers. For a hollow-core fiber with eight capillaries in the cladding, we can observe a strong vortex motion of the orbital part vector at the boundaries of the cladding capillaries, which, apparently, is directly related to a sharp decrease in the loss level in such hollow-core fibers.

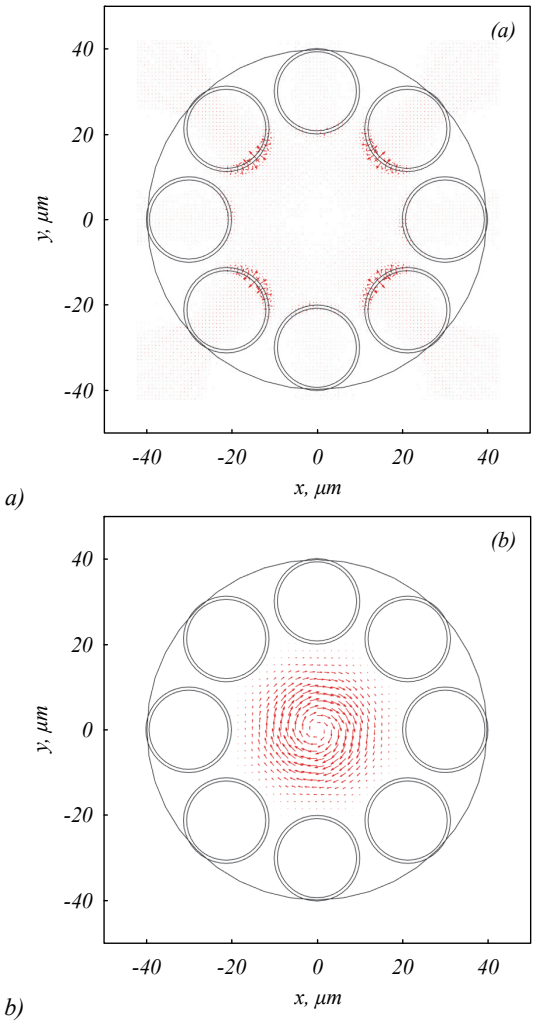

Fig. 5. a) Distribution of the orbital part of the transverse component of the Poynting vector of HE_{21} air-core mode of the silica glass hollow-core fiber for the case of linear polarization at wavelength of 1 μm; (b) distribution of the orbital part of the transverse component of the Poynting vector of HE_{21} air-core mode of the silica glass hollow-core fiber for the case of circular polarization at the same wavelength

In our future work, we plan to carry out additional studies that will possibly allow us to find a mechanism for reducing losses in hollow-core fibers based on the complex vortex behavior of the transverse energy flow of the air-core modes.

Acknowledgements

The work was funded Russian Science Foundation under project # 22-22-00575.

References

[1] Zhuo W, Jiajing T, Shecheng G, Zhaohui L, Changyuan Y, Chao L. Transmission and generation of orbital angular momentum modes in optical fibers. Photonics 2021; 8: 246. DOI: 10.3390/photonics8070246.

[2] Bozinovic N, Yue Y, Ren Y, Tur M, Kristensen P, Huang H, Willner AE, Ramachandran S. Terabit – scale orbital angular momentum mode division multiplexing in fibers. Science 2013; 340: 1545-1548. DOI: 10.1126/science.1237861.

[3] Willner AE, Huang H, Yan Y, Ren Y, Ahmed N, Xie G, Bao C, Li L, Cao Y, Zhao J, Wang J, Lavery MPJ, Tur M, Ramachandran S, Molisch AF, Ashrafi N, Ashrafi S. Optical communications using orbital angular momentum beams. Adv Opt Photonics 2015; 7: 66-106. DOI: 10.1364/AOP.7.000066.

[4] Gregg P, Kristensen P, Ramanchandran S. Conservation of orbital angular momentum in air-core optical fibers. Optica 2015; 2: 267-270. DOI: 10.1364/OPTICA.2.000267.

[5] Gregg P, Kristensen P, Ramanchandran S. 13.4 km OAM state propagation by recirculating fiber loop. Opt Express 2016; 24: 18938-18947. DOI: 10.1364/OE.24.018938.

[6] Li H, Ren G, Gao Y, Zhu B, Wang J, Yin B, Jian S. Hollow – core photonic band gap fibers for orbital angular momentum applications. J Opt 2017; 19: 045704. DOI: 10.1088/2040-8986/aa612c.

[7] Li H, Ren G, Zhu B, Gao Y, Yin B, Wang J, Jian S. Guiding terahertz orbital angular momentum beams in multi-mode Kagome hollow-core fibers. Opt Lett 2017; 42: 179-182. DOI: 10.1364/OL.42.000179.

[8] Zhang J, Lin Z, Liu J, Liu J, Lin Z, Mo S, Lin S, Shen L, Zhang L, Chen Y, Lan X, Yu S. SDM transmission of orbital angular momentum mode channels over a multi-ring-core fibre. Nanophotonics 2022; 11: 873-884. DOI: 10.1515/nanoph-2021-0471.

[9] Xi XM, Wong GKL, Frosz MH, Babic F, Ahmed G, Jiang X, Euser TG, Russell PStJ. Orbital-angular-momentum-preserving helical Bloch modes in twisted photonic crystal fiber. Optica 2014; 1: 165-169. DOI: 10.1364/OPTICA.1.000165.

[10] Russell PStJ. Photonic-crystal fibers. J Lightw Technol 2006; 24: 4729-4749. DOI: 10.1109/JLT.2006.885258.

[11] Pryamikov AD, Biriukov AS, Kosolapov AF, Plotnichenko VG, Semjonov SL, Dianov EM. Demonstration of a waveguide regime for a silica hollow – core microstructured optical fiber with a negative curvature of the core boundary in the spectral region > 3.5 μm. Opt Express 2011; 19: 1441-1448. DOI: 10.1364/OE.19.001441.

[12] Pryamikov AD, Alagashev GK, Falkovich G, Turitsyn S. Light transport and vortex-supporting wave-guiding in micro-structured optical fibers. Sci Rep 2020; 10: 2507. DOI: 10.1038/s41598-020-59508-z.

[13] Volyar AV, Fadeeva TA. Angular momentum of the fields of a few-mode fiber: I. A perturbed optical vortex. Tech Phys Lett 1997; 23: 848-851. DOI: 10.1134/1.1261907.

[14] Alagashev G, Stafeev S, Kotlyar V, Pryamikov A. The effect of the spin and orbital parts of the Poynting vector on light localization in solid-core micro-structured optical fibers. Photonics 2022; 9: 775. DOI: 10.3390/photonics9100775.

[15] Alagashev G, Stafeev S, Kotlyar V, Pryamikov A. Angular momentum of leaky modes in hollow-core fibers. Fibers 2022; 10(10): 92. DOI: 10.3390/fib10100092.

[16] Berry MV. Optical currents. J Opt 2009; 11: 094001. DOI: 10.1088/1464-4258/11/9/094001.

[17] Ramachandran S, Kristensen P. Optical vortices in fiber. Nanophotonics 2013; 2: 455-474. DOI: 10.1515/nanoph-2013-0047.

Authors' information

Grigory Konstantinovich Alagashev, (b. 1989). Graduated from the Moscow Institute of Physics and Technology in 2013. Junior Research Fellow at Prokhorov General Physics Institute of Russian Academy of Sciences. Research interests: fiber optics, microstructured light guides, mathematical modeling.
E-mail: *alagashevgrigory@gmail.com* ORCID: 0000-0001-7654-7860.

Sergey Sergeevich Stafeev (b. 1985) received Master's degree in Applied Mathematics and Physics in Samara State Aerospace University (2009). He received his PhD in 2012. He is researcher of Laser Measurements laboratory at the Image Processing Systems Institute, NRC "Kurchatov Institute". Scientific interests: diffractive optics, FDTD method, nearfield optics. E-mail: *sergey.stafeev@gmail.com* ORCID: 0000-0002-7008-8007.

Andrey Dmitrievich Pryamikov, (b. 1975). He graduated from Physics faculty of the Moscow State University M. V. Lomonosov in 1999. He received his PhD in 2002. Senior Researcher at Prokhorov General Physics Institute of Russian Academy of Sciences (Laboratory of Spectroscopy). Research interests: microstructured optical fibers, non-linear fiber optics, photonic crystals, optical microcavities. E-mail: *pryamikov@mail.ru* ORCID: 0000-0003-2808-7040.

Code of State Categories Scientific and Technical Information (in Russian – GRNTI)): 47.35.41
Received May 19, 2023. The final version – July 6, 2023.